Int. J. Electrochem. Sci., 15 **(2020)** 6155 – 6164, doi: 10.20964/2020.07.15

International Journal of
ELECTROCHEMICAL
SCIENCE
www.electrochemsci.org

Short Communication

Hydrothermal Fabricated Ag Nanoparticles-decorated Reduced Graphene Oxide Composite for H_2O_2 Electrochemical Detection

Shuisheng Wu[*], *Nianyuan Tan, Donghui Lan, Chak-Tong Au and Bing Yi*[*]

Hunan Provincial Key Laboratory of Environmental Catalysis & Waste Recycling, School of Materials and Chemical Engineering, Hunan Institute of Engineering, Xiangtan 411104, China
[*]E-mail: wuss_2005@126.com (S.W.), bingyi2004@126.com (B.Y.)

Received: 8 March 2020 / *Accepted:* 20 April 2020 / *Published:* 10 June 2020

Composite made up of silver nanoparticles and reduced graphene oxide (AgNPs-rGO) has been successfully prepared through a simple one-pot hydrothermal method using sodium borohydride as reducing agent. The structure and morphology of AgNPs-rGO have been characterized by XRD, FTIR, Raman and TEM techniques. It was observed that this composite material shows good catalytic activity for the electrochemical detection of hydrogen peroxide (H_2O_2). In the H_2O_2 concentration range of 1.0×10^{-6}–1.2×10^{-3} mol/L, the electrochemical current of AgNPs-rGO/CPE increases linearly with the concentration of H_2O_2 (R^2 = 0.9974). The results show that the prepared AgNPs-rGO has good stability and performance reproducibility for H_2O_2 detection based on electrochemical analysis.

Keywords: Reduced graphene oxide; Silver nanoparticles; Hydrogen peroxide; Electrochemical detection, Hydrothermal synthesis

1. INTRODUCTION

Hydrogen peroxide (H_2O_2) is an important industrial intermediate and medical disinfectant, and has been widely used in environmental, pharmaceutical, and food industries [1]. However, a high concentration of H_2O_2 is hazardous to the environment and human health [2]. Therefore it is of significance to develop a method that is rapid, sensitive and effective for H_2O_2 detection [3]. At present the methods for H_2O_2 detection mainly based on chemiluminescence [4], fluorescence [5], spectrophotometry [6], and electrochemistry [7]. Among them, the electrochemical method has the advantages of high sensitivity as well as operational simplicity and rapidity [8].

With good biocompatibility, electrical conductivity and catalytic properties, silver nanoparticles (AgNPs) have wide applications in various fields [9], and have been used in electrochemical detection of H_2O_2. However, the main drawback of AgNPs is poor stability in aqueous solution as a result of

agglomeration [10]. Especially during repeated charge-discharge electrode processes, agglomeration of AgNPs is highly likely, leading to decrease of electrochemical performance [11]. It is hence of great significance to enhance the stability of AgNPs through agglomeration prevention in electrochemical applications. Graphene is a versatile material widely used in many fields due to positive factors such as large specific surface area, excellent optoelectronic properties, catalytic ability, as well as good biocompatibility and stability [12]. Furthermore, the chemically reduced graphene oxide (rGO) is large in specific surface area and rich in carbon-oxygen functional groups, and has been used as support for AgNPs to circumvent the problem of agglomeration [13–16]. However, most of the developed methods for the synthesis of AgNPs/rGO involve multiple steps, and when comes to high silver content, dispersibility is poor. It is still a challenge to develop a simple method for efficient preparation of AgNPs/rGO hybrids with high silver content and good dispersion.

In this paper, AgNPs-rGO composites were prepared by using rGO and silver nitrate as raw materials. The anchoring of AgNPs on the graphene of large specific surface area enables uniform distribution of AgNPs, which effectively prevents the agglomeration of AgNPs and enhances the catalytic and stability of AgNPs. Then it was made into an AgNPs-rGO/CPE, and the electrode was applied for electrochemical detection of H_2O_2. With the establishment of linear relation between H_2O_2 concentration and response current, the electrochemical analysis method is apt for H_2O_2 detection. Furthermore, the stability and anti-interference ability of the method were studied.

2. MATERIALS AND METHOD

2.1 Reagents and instruments

Graphite powder, silver nitrate, excellent purity grade, Sinopharm reagent company; sodium borohydride, sulfuric acid, sodium citrate, dimethicone, potassium chloride, analytically pure, Guangzhou Chemical Reagent Factory. CHI760e electrochemical analyzer: Shanghai Chenhua Instrument Company; IM-6ex type electrochemical workstation: ZAHNER, Germany; D8 ADVANCE X-Ray Diffractometer: Bruker, Germany; Hirox SH-5000M scanning electron microscope: Phenom, Netherlands.

2.2 Material preparation

GO was prepared by the modified Hummers method [17]. The AgNPs-rGO composite was synthesized by a simple one-step reduction wet chemical process. The specific steps are as follows: 10 mg of GO and 40 mg of sodium citrate were added to 50 mL of deionized water, and the mixture was subject to stirring of 1 h for even dispersion. Then 2 mL of 0.02 mol/L silver nitrate solution was added with constant stirring for 15 min. Subsequently, 5 mL of 8 g/L sodium borohydride solution was added followed by stirring of 1 h. The as-resulted mixture was transferred to a 100 mL hydrothermal autoclave, and subject to hydrothermal treatment at 180 ℃ for 12 h. The produced black solid was collected by vacuum filtration and dried at 60 ℃ to obtain AgNPs-rGO. Silver-graphene doped carbon paste electrode (AgNPs-rGO/CPE) used in the study was prepared by a specific method which is as follows: 0.1 g of prepared AgNPs-rGO and 0.9 g of polished graphite powder were uniformly mixed. Then 100 μL of

dimethyl silicone oil was added dropwise into the mixture, which was stirred and compressed into a homogeneous paste. The paste was filled into a glass tube having a diameter of ca. 4 mm and was compacted, and then a copper wire was inserted into the paste, which was used after self-test over the electrochemical workstation. The working electrode was stored at room temperature and kept away from light. Meanwhile, rGO/CPE (a carbon paste electrode doped with rGO) and CPE (a carbon paste electrode without any doping) were also prepared for comparison purposes.

2.3. Electrochemical test

Cyclic voltammetry tests were carried out in three-electrode electrolytic cells at room temperature, using platinum plate as auxiliary electrode, and Ag/AgCl (Saturated KCl) as reference electrode. For H_2O_2 reduction tests, the experiment was carried out under the protection of N_2. AgNPs-rGO/CPE was used as the working electrode, and cyclic voltammetry scan was performed in the potential range of 0.6 to -0.2 V. The H_2O_2 solution used in the experiment was newly prepared every day, and 0.02 M phosphate buffer solution (PBS, pH=5.5) was used in the test.

The chronoamperometric test was performed by applying an external potential of -0.5V with continuous addition of a certain concentration of H_2O_2 in the buffer solution under magnetic stirring. The minimum detection limit was analyzed by fitting the relationship between the concentration of H_2O_2 and response current.

3. RESULTS AND DISCUSSION

3.1 Material characterization

To verify the crystal structure and phase purity of GO, rGO and AgNPs-rGO, samples of the materials were characterized by X-ray diffractometry (XRD), and the results are shown in Figure 1. Due to the large number of defects and oxygen-containing groups in GO, the characteristic (001) peak of GO appeared at 11.8°. After reduction by sodium borohydride, the GO characteristic peak disappeared, and a broad peak appeared at 24.2°, indicating that GO was reduced to rGO with an ordered crystal structure [18]. By comparison with the JCPDS standard card, it was found that the diffraction peaks of AgNPs-rGO at 38.1°, 44.3°, 64.4°, and 77.4° are consistent with those of Ag cubic phase, corresponding to (111), (200), (220), and (311) crystal planes (JCPDS No. 04-0783) [19]. The characteristic peak of rGO at 24.2° is also observed in the pattern of the AgNPs-rGO composite. This indicates that AgNPs has been successfully loaded on the surface of rGO. There were no other diffraction peaks in the synthesized sample, indicating that the sample was of high purity and did not contain any impurities.

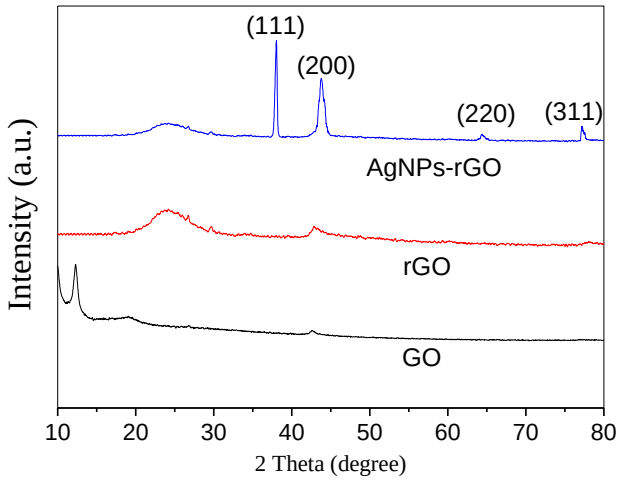

Figure 1. XRD spectra of GO, rGO and AgNPs-rGO

Figure 2 shows the FT-IR spectra of the GO and AgNPs-rGO samples. Over GO, the absorption peak at 1612 cm^{-1} is due to carbon skeleton stretching vibration whereas those at 1722, 1612, 1226, and 1046 cm^{-1} ascribable to stretching vibration of C=O, C=C, C-OH, and C-O-C, respectively [20]. Over the AgNPs-rGO sample, the C=O peak at 1722 cm^{-1} disappeared, and the C-O-C and C-OH peaks weakened, indicating reduction of oxygen-containing groups in GO by sodium borohydride [21].

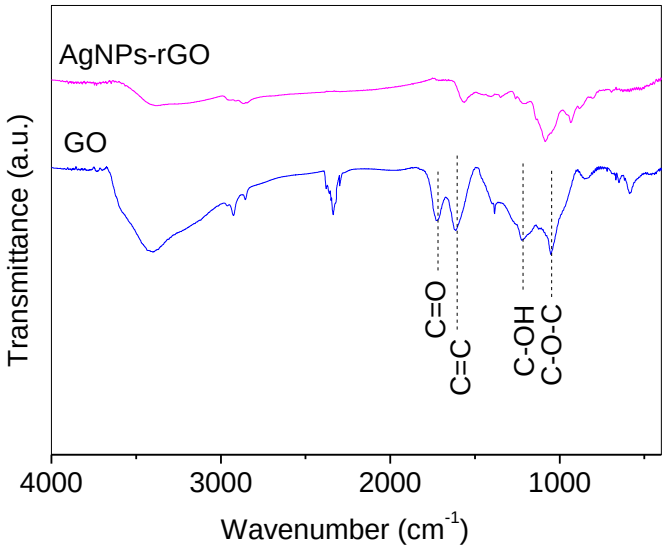

Figure 2. FT-IR spectra of GO and AgNPs-rGO

Raman spectroscopic investigation of GO and AgNPs-rGO were conducted to characterize the molecular structure (Fig. 3). Over both GO and AgNPs-rGO, a G band at 1 595 cm^{-1} corresponding to sp hybrid carbon atoms and a D band at 1352 cm^{-1} attributable to disordered carbon atoms were observed.

The peak intensity ratio (I_D/I_G) of D band to G band of the AgNPs-rGO composite is 1.08, which is higher than that of GO (I_D/I_G = 0.93). The results indicate that there is higher among of disordered carbon atoms in AgNPs-rGO, plausibly a result of having the silver NPs anchored on the graphene surface [22].

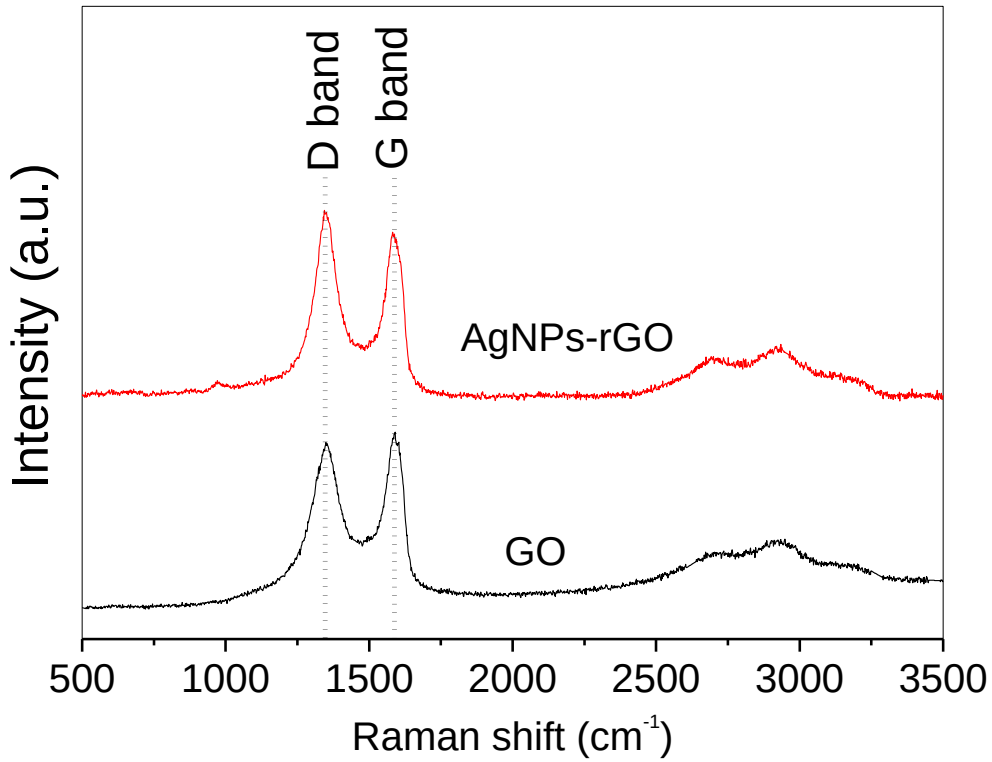

Figure 3. Raman spectra of GO and AgNPs-rGO

The morphology of GO and AgNPs-rGO materials was characterized by TEM. In Fig. 4a, GO exhibits a smooth surface with yarn-like folds, indicating that GO has a two-dimensional flat structure composed of a small number of layers. As can be seen from Figure 4b, the surface of the AgNPs-rGO material still maintains a good graphene layered structure, and there are AgNPs with size ranging from 15 to 20 nm uniformly dispersed on the graphene surface. It is apparent that due to the interaction between AgNPs and graphene surface, the AgNPs do not undergo agglomeration. Elemental characterization of AgNPs-rGO by EDX confirms the presence of carbon, oxygen, and silver (Fig. 4c), in agreement with the existence of rGO and AgNPs in the composite. The inset of Figure 4c is a mass distribution diagram of the detected elements contained in AgNPs-rGO. The mass fraction of silver is 51.5%. Compared with some AgNPs-graphene composites reported in literatures [23, 24], the AgNPs-rGO of this paper is higher in Ag loading.

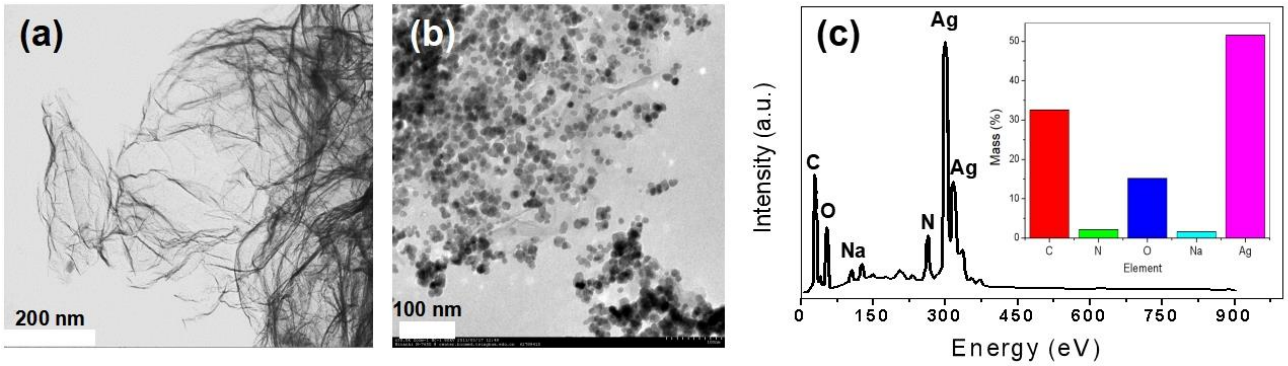

Figure 4. (a) TEM image of GO; (b) TEM image of AgNPs-rGO; and (c) EDX of AgNPs-rGO

3.2 Electrochemical research

The electrochemical performance of CPE, rGO/CPE and AgNPs-rGO/CPE was examined by cyclic voltammetry using potassium ferricyanide ($K_3[Fe(CN)_6]$) as standard substance in 0.02 M PBS buffer at pH = 5.5. The results are shown in Fig. 5, all three electrodes show obvious electrochemical signals in $K_3[Fe(CN)_6]$. With the modification of rGO and finally rGO and Ag NPs, the oxidation peak current and the reduction peak current gradually increase, indicating that the presence of rGO and AgNPs can promote the electron transfer speed of electrode, leading to enhanced electrochemical response. Among them, AgNPs-rGO/CPE is the highest in response current (Fig. 5A). Fig. 5B illustrates the cyclic voltammetry charts of the three electrodes after adding 10^{-5} mol/L H_2O_2. The response current of CPE is very small whereas that of rGO/CPE is good, and that of AgNPs-rGO/CPE is even better. The results indicate that AgNPs-rGO has a significant promotion effect on the electrochemical response in the detection of H_2O_2. This is attributed to two effects: First, due to the large specific surface area of AgNPs-rGO, the generation of AgNPs-rGO/CPE would expand the electrode area, providing more electrochemical sites as a consequence. Second, AgNPs-rGO has good electrical conductivity and the cooperative catalysis of AgNPs and rGO lowers the energy barrier of the reaction. The overall outcome is good electrocatalytic activity of electrode, which is consistent with literature report [25].

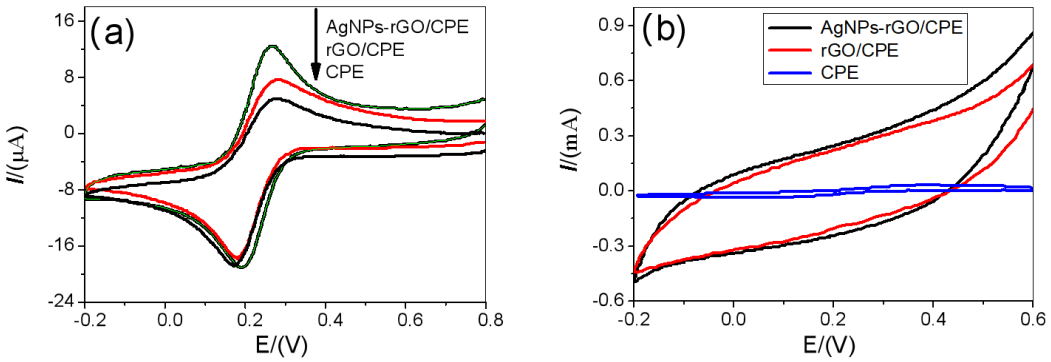

Figure 5. Cyclic voltammograms (CV) of CPE, rGO/CPE and AgNPs-rGO/CPE with (A) 10^{-5} mol/L $K_3[Fe(CN)_6]$ and (B) 10^{-5} mol/L H_2O_2 in 0.02 M PBS at pH=5.5) with scan rate of 50 $mV \cdot s^{-1}$

The time-current (*I-t*) curve is an important means for the acquisition of electrochemical linear range. Fig. 6 depicts the *I-t* curves collected over the three electrodes. It can be seen that over CPE, there is little change of current value with the addition of H_2O_2, while the electrode currents in the cases of rGO/CPE and AgNPs-rGO/CPE have obvious responses with the change of H_2O_2 concentration, confirming that rGO and AgNPs are good for electrochemical sensing of H_2O_2. It is noted that the speed of current response over AgNPs-rGO/CPE is higher than that over rGO/CPE, implying well dispersion of AgNPs on graphene surface would lead to enhanced conductivity and catalytic performance. Thus, AgNPs-rGO/CPE is superior to rGO/CPE and CPE in terms of H_2O_2 detection. The inset of Fig. 6 discloses the current change over AgNPs-rGO/CPE in three times of detection upon H_2O_2 addition of 10^{-5} mol/L. The current responses in the three tests were -7.1, -7.24, and -7.03 μA, respectively, giving a relative standard deviation RSD of only 2.7%. The results indicate good stability and performance reproducibility of AgNPs-rGO/CPE in electrochemical H_2O_2 detection.

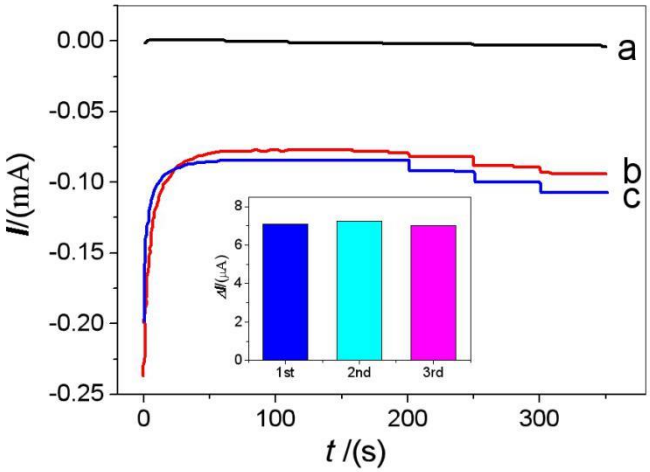

Figure 6. *I-t* curves of H_2O_2 in 0.02 M PBS (pH=5.5) over **a**: CPE, **b**: rGO/CPE, and **c**: AgNPs-rGO/CPE; (The inset displays the ΔI values over AgNPs-rGO/CPE in three times of detection)

3.3 H_2O_2 detection and application

The detection results are shown in Fig. 7. The best condition for H_2O_2 detection was in a PBS of pH=5.5 and at an external potential of -0.5V. It can be seen from Fig. 7a that the response current over AgNPs-rGO/CPE is closely related to H_2O_2 concentration, and with the decrease of H_2O_2 concentration, there is gradual increase of current change (ΔI). As depicted in Fig. 7b, there is a good linear relationship between the logarithm of concentration (lg$c$) and ΔI in the H_2O_2 concentration range from 1×10^{-6}– to 1×10^{-3} mol/L. The linear equation is $\Delta I = 0.01411 \times \lg c + 0.085$, and the correlation coefficient R^2 is 0.9974. With such excellent linear correlation, an electrochemical method for H_2O_2 detection can be established, and the minimum detection limit is 3.4×10^{-7} mol/L.

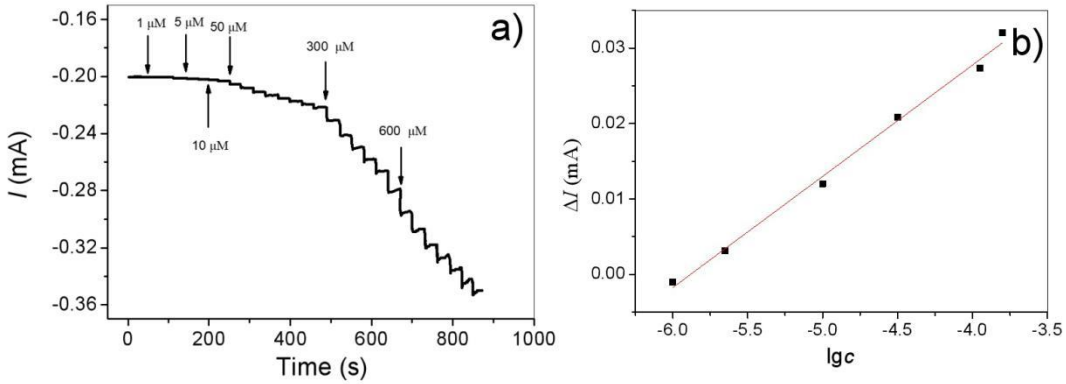

Figure 7. (a) *I-t* curves of H_2O_2 at different concentrations over AgNPs-rGO/CPE in 0.02 M PBS (pH 5.5) and (b) linear relationship between lg*c* and Δ*I*

Electrochemical H_2O_2 detection performance of AgNPs-rGO/CPE has been compared with those of H_2O_2 sensors reported in literatures (Table 1). It is apparent that the electrode synthesized in the present study is superior to the others when both linear range and detection limit is put into consideration.

Table 1. Electrochemical H_2O_2 sensing performances of different electrodes

Modified electrode	Linear range, c/(μmol/L)	LOD[a], c/(μmol/L)	Ref.
PB/rGO-CS/GCE	10–400	0.213	[26]
Ag nanowire/GC	50–10350	10	[27]
AgNPs-MWCNT/Au	50–17000	0.5	[28]
Cu-Co dendrite/GC	1.0–11000	0.75	[29]
CNs /Fe_3O_4/GC	1–1000	0.66	[30]
Ag-rGO/CPE	100–7000	2.04	[16]
AgNPs-rGO/CPE	1–1000	0.34	This work

[a] LOD stands for limit of detection.

It is generally considered that stability and anti-interference ability are important factors for the evaluation of an analytical method. Fig. 8 is the *I-t* curve of H_2O_2 detection by AgNPs-rGO/CPE upon the addition of various interfering substances. It can be seen that after the addition of H_2O_2, there is significant reduction of current, revealing the super sensitivity of AgNPs-rGO/CPE toward H_2O_2. Upon the addition of potassium nitrate, sodium chloride, ascorbic acid (AA), and glucose (Glu), there is almost no current change, indicating that the analytical method is free from the interference of these common substances. Gratifyingly, when H_2O_2 is added again, the drop of current occurs again, confirming that the electrochemical response of AgNPs-rGO/CPE is not affected by the presence of these substances, indicating that the AgNPs-rGO complex has good stability and performance reproducibility. The results show that the electrode described in this paper has good anti-interference ability and stability, which is conducive to the actual detection of H_2O_2.

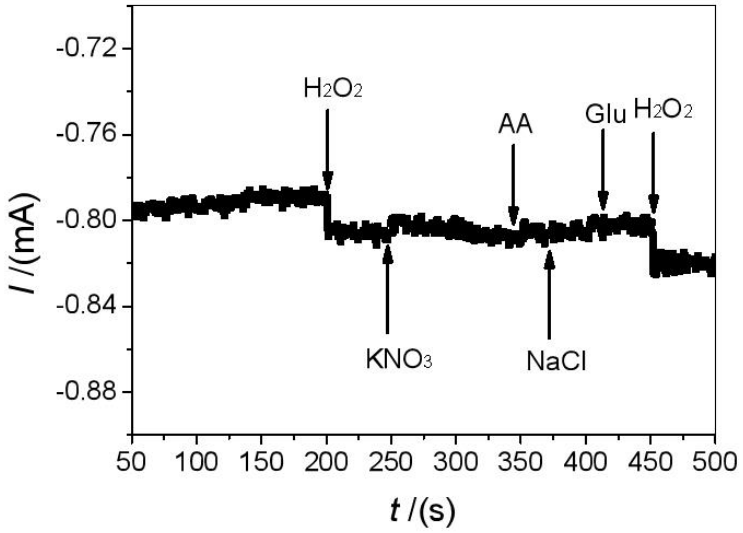

Figure 8. *I-t* curve of observed over AgNPs-rGP/CPE in 10^{-5} mol/L H_2O_2 upon the addition of KNO_3, AA, NaCl and Glu in 0.02 M PBS (pH 5.5) (The concentration of KNO_3, NaCl, Glu and AA addition was 10^{-4} mol/L)

In order to assess the applicability of the prepared electrochemical sensor, we selected a sample of tap water as analysis object. In the test, AgNPs-rGO/CPE was used, and hydrogen peroxide in the sample was analyzed following the described procedure. The results show that the spike recovery of H_2O_2 reaches 97.6%, and the relative standard deviation of multiple data is 4.8%. Moreover, the results obtained by this method are basically consistent with those obtained by traditional potassium permanganate titration method [31]. This indicates that AgNPs-rGO/CPE exhibits good stability and reproducibility in electrochemical detection of H_2O_2, and can be used for the analysis and detection of H_2O_2 in actual samples.

4. CONCLUSION

In this work, AgNPs/rGO composite with high silver content and well-dispersed AgNPs were synthesized by a simple hydrothermal method using sodium borohydride as reducing agent. The AgNPs/rGO hybrid was successfully applied in the non-enzymatic detection of H_2O_2. The AgNPs-rGO/CPE displays a linear relationship in a wide H_2O_2 concentration range (from 1×10^{-6} to 1×10^{-3} mol/L; R^2 = 0.9974), showing a minimum detection limit of 3.4×10^{-7} mol/L. The results demonstrate that with the use of rGO, the analytical method has good stability and spike recovery, and can be repeatedly applied for the detection of H_2O_2 in actual samples.

ACKNOWLEDGEMENTS
This project was supported by the National Natural Science Foundation of China (21772035), the Scientific Research Fund of Hunan Provincial Education Department (19B126), the Talent Research Startup Fund of Hunan Institute of Engineering (18RC009), the Open Fund Hunan Province Key

Laboratory of Environmental Catalysis and Waste Recycling (2018KF06) and Pre-Research Science Fund Project of Hunan Institute of Engineering (YY1906).

References

1. K. Dhara and D. R. Mahapatra. *J. Mater. Sci.*, 54(2019) 12319–12357.
2. C. Tredwin, S. Naik, N. Lewis and C. Scully. *Br. Dent. J*, 200(2006) 371–376.
3. Z. Zhao, Q. Ou, X. Yin and J. Liu. *Int. J. Biosens. Bioelectron*, 2(2007) 25–28.
4. X. Q. Tang, Y. D. Zhang, Z. W. Jiang, D. M. Wang, C. Z. Huang and Y. F. Li. *Talanta*, 179(2018) 43–50.
5. R.Tian, B.Zhang, M.Zhao, Q.Ma and Y. Qi. *Talanta*, 188(2018) 332–338.
6. D. Wang, S. Qiu, M. Wang, S. Pan, , H. Ma and J. Zou. *Spectrochimica Acta A*, 221(2019) 117138.
7. L. Wang and E. Wang. *Electrochem. Commun.*, 6(2004) 225–229.
8. H. Song, H. Zhao, X. Zhang, Y. Xu, X. Cheng, S. Gao and L. Huo. *Microchimica Acta*, 186(2019) 210.
9. L. Balan, J. P. Malval, R. Schneider, and D. Burget. *Mater. Chem. Phys.*, 104 (2007) 417–421.
10. E. McGillicuddy, I. Murray, S. Kavanagh, L. Morrison, A. Fogarty and M. Cormican. *Sci. Total Environ.*, 575(2017) 231–246.
11. S. Duan, Y. Rui and Y. Huang. *Talanta*, 160(2016) 607–613.
12. V. B. Mohan, K. Lau, D. Hui and D. Bhattacharyya. *Compos. Part B-Eng.*, 142(2018) 200–220.
13. L. Zhang, Q. Tan , H. Kou, D. Wu, W. Zhang, and J. Xiong. *Sci. Rep.*, 9(2019) 1–10.
14. B. Fan, Y. Li, F. Han, T. Su, J. Li and R. Zhang. *J. Mater. Sci. Mater. M.*, 29(2018) 69.
15. M. Y. Wang, T. Shen, M. Wang, D. E. Zhang and J. Chen. *Mater. Lett.*, 107 (2013) 311–314.
16. B. Yu, J. C. Feng, S. Liu and T. Zhang. *RSC Adv.*, 3(2013) 14303–14307
17. P. Kumar, S.Penta and S. P. Mahapatra. *Integr. Ferroelectr.*, 202(2019) 41–51.
18. G. Kazuma, K. Tara, J. Eiji, Y. Aki, H. Hideki, O. Takahiro, I. Atsushi, K. Yasushige and I. Hiroyuki. Carbon, 49(2011) 1118–1125.
19. J. Li and C. Liu. *Eur. J. Inorg. Chem.* 2010(2010) 1244–1248.
20. C. H. Manoratne, S. R. D. Rosa and I. R. M. Kottegoda . *Mater. Sci. Res. India*, 14(2017) 19–30.
21. X. Y. Yang, X. B. Wang, J. Li, J. Yang, L. Wan and J. C. Wang. *Chem. J. Chinese U.*, 33(2012) 1902–1907.
22. C. He, Z. Liu, Y. Lu, L. Huang and Y. Yang. *Int. J. Electrochem. Sci.*, 11(2016) 9566–9574.
23. Z. Meng, B. Liu and M. Li. *Int. J. Electrochem. Sci.*, 12(2017) 10269–10278.
24. Y. Wei ,X. Zuo , X. Li , S. Song, L. Chen, J. Shen,Y. Meng, Y. Zhao and S. Fang. *Mater. Res. Bull.*, 53(2014) 145–150.
25. X. X. Liu, X. W. Xu, H. Zhu and X. R. Yang. *Anal. Methods*, 5(2013) 2298–2304.
26. H. Yang, N. Myoung and H. G. Hong. *Electrochim. Acta*. 81(2012) 37–43
27. W. H. Hsiao，H. Y.Chen and T. M. Cheng. *J Chin. Chem. Soc.*, 59(2012) 500
28. W. Zhao, H. Wang, X. Qin, X. Wang, Z. Zhao, Z. Miao, L. Chen, M. Shan, Y. Fang and Q. Chen. *Talanta*, 80 (2009) 1029–1033
29. H. B. Noh, K. S. Lee, P. Chandra, M. S. Won and Y. B. Shim. *Electrochim. Acta*, 61(2012) 36–43
30. S. Y.Zhang，H. J.Wang，S. F. Li and J. Y. Ying. *J. Electrochem.*, 24(2018) 279–283
31. L. Chen, X. Xu, F. Cui,Q. Qiu, X. Chen and J. Xu. *Anal. Biochem.*, 554(2018) 1–8.